



FACULTY OF ENGINEERING
ALEXANDRIA UNIVERSITY

Alexandria University
Alexandria Engineering Journal

www.elsevier.com/locate/aej
www.sciencedirect.com



ORIGINAL ARTICLE

Numerical simulation of double diffusive laminar mixed convection in shallow inclined cavities with moving lid

Mohamed A. Teamah ^{a,b,*}, Medhat M. Sorour ^a, Wael M. El-Maghlany ^a,
Amr Affi ^a

^a Mechanical Engineering Department, Alexandria University, Alexandria, Egypt

^b Mechanical Engineering Department, Arab Academy for Science, Technology and Maritime Transport, Alexandria, Egypt

Received 1 April 2012; revised 24 January 2013; accepted 2 February 2013
Available online 9 March 2013

KEYWORDS

Heat and mass transfer;
Inclined cavities;
Double-diffusive flow;
Mixed convection;
Lid driven cavity;
Numerical simulation

Abstract A numerical investigation of double-diffusive laminar mixed convection in an inclined cavity has been studied numerically. The top lid was considered to move in both directions to introduce the forced convection effect. In addition, the solutal and thermal buoyancy forces are sustained by maintaining the top lid and the bottom surface at uniform temperatures and concentrations, but their values for the top lid are higher than those at the bottom surface. The laminar flow regime is considered under steady state conditions. Moreover, the transport equations for continuity, momentum, energy and mass transfer are solved. The streamlines, isotherms and isoconcentrations as well as both local and average Nusselt and Sherwood numbers were studied for the hot lid. The effects of inclination of the cavity on the flow, thermal and mass fields are investigated for inclination angles ranging from 0° to 30°. The study covers a wide range for $0.1 \leq Le \leq 10$ and $-10 \leq N \leq 10$. Through this investigation, the following parameters are kept constant: The aspect ratio at 10, Prandtl number at six representing water. A comparison was made with published results and a good agreement was found.

© 2013 Production and hosting by Elsevier B.V. on behalf of Faculty of Engineering, Alexandria University.

1. Introduction

In the past three decades a lot of interest has been given to the heat transfer in fluid filled cavities. Numerous investigations have been conducted in the past on lid-driven cavity flow and heat transfer considering various combinations of the imposed temperature gradients and cavity configurations. This is because the driven cavity configuration is encountered in many practical engineering and industrial applications. Convection plays a dominant role in crystal growth (e.g., [1–4]) in which it affects the fluid-phase composition and temperature at the phase interface that results in a single crystal since poor crystal

* Corresponding author at: Mechanical Engineering Department, Alexandria University, Alexandria, Egypt. Tel.: +20 1003969521; fax: +20 35921853.
E-mail address: mteamah@yahoo.com (M.A. Teamah).
Peer review under responsibility of Faculty of Engineering, Alexandria University.



Production and hosting by Elsevier

Nomenclature

A	aspect ratio of the cavity, L/H	Ri	Richardson number, $Ri = Gr/Re^2$
c	concentration, kg/kg _f	Sc	Schmidt number, $Sc = \nu/D$
c_h	concentrations at the hot surface (lid) of the cavity, kg/kg _f	Sh	average Sherwood number, $Sh = h_s H/D$
c_l	concentrations at the cold surface of the cavity, kg/kg _f	Sh_x	local Sherwood number
C	dimensionless concentration, $C = (c - c_l)/(c_h - c_l)$	T	local temperature, K
Δc	concentration difference, $c_h - c_l$	T_c	temperature of the cold surface, K
D	mass diffusivity, m ² /s	T_h	temperature of the hot surface (lid), K
g	gravitational acceleration, m s ⁻²	ΔT	temperature difference, $T_h - T_c$, K
Gr	Grashof number based on cavity height, $Gr = g\beta_T (T_h - T_c)H^3/\nu^2$	u	velocity components in x -direction
h_T	heat transfer coefficient, W m ⁻² K ⁻¹	U_{lid}	lid velocity, m/s
h_s	solutal transfer coefficient, m s ⁻¹	v	velocity components in y -direction
H	height of the cavity, m	V	dimensionless velocity component in Y -direction
k	thermal conductivity of fluid, W m ⁻¹ K ⁻¹	x, y	dimensional coordinates
L	length of the cavity, m	X, Y	dimensionless coordinates
Le	Lewis number, $Le = \alpha/D = Sc/Pr$	<i>Greek symbols</i>	
N	buoyancy ratio, $N = \beta_S \Delta c / \beta_T \Delta T$	α	thermal diffusivity, m ² /s
Nu	average Nusselt number, $Nu = h_T H/k$	β_T	coefficient of thermal expansion, K ⁻¹
Nu_x	local Nusselt number	β_S	coefficient of solutal expansion, m ³ /kg
p	pressure, N/m ²	γ	cavity inclination angle
P	dimensionless pressure, $P = p/\rho_\infty u_{lid}^2$	θ	dimensionless temperature, $(T - T_c)/(T_h - T_c)$
Pr	Prandtl number, $Pr = \nu/\alpha$	μ	dynamic viscosity, kg/m s
Ra	Rayleigh number, $Ra = GrPr$	ρ	local Fluid density, kg/m ³
Re	Reynolds number based on cavity height, $Re = u_{lid}H/\nu$	ρ_∞	fluid density at the bottom surfaces, kg/m ³
		ν	kinematics viscosity, m ² /s

quality is due to turbulence. It is the foundation in modern electronics industry to produce pure and perfect crystals to make transistors, lasers rods, microwave devices, infrared detectors, memory devices, and integrated circuits. The analysis of lid-driven cavity flow and heat transfer considering various combinations of the imposed temperature gradients and cavity configurations is important because the resulting flow however, is rather complex even when the flow is purely shear driven for the isothermal case without any temperature gradient. When a temperature gradient is imposed such that the shear driven and buoyancy effects are of comparable magnitude then the resulting flow falls under the mixed convection regime and the interaction and coupling of these effects makes the analysis more complex. The combination of temperature and concentration gradients in the fluid will lead to double-diffusive flows. This has an important influence on the solidification process in a binary system [5] and oceanography [6]. Hyun and Lee [7] have reported numerical solutions for double-diffusive convection in a rectangular enclosure with aiding and opposing temperature and concentration gradients. Their solutions were compared favorably with reported experimental results. Most of the studies performed on natural convection heat transfer inside enclosed spaces are related to unidirectional heat flows across rectangular cavities, wherein the buoyancy is induced by imposing a heat flux or a temperature difference either horizontally or vertically from below, in examining conventional convection or thermal instabilities, respectively. Detailed reviews on this topic are easily available in the literature, such as those by Ganzarolli and Milanez [8]

and Basak et al. [9]. The natural convection in a two dimensional cavity with vertical cavity walls are maintained at constant and uniform different levels of temperature and two adiabatic walls which analyzed by Loa et al. [10] and Costa [11]. Aydin et al. [12] investigated the effect of Rayleigh number and aspect ratio in two-dimensional enclosure isothermally heated from the left and cooled from the ceiling while the other side wall and the floor are perfectly insulated. Iwatsu and Hyun [13] also carried three-dimensional numerical simulations of fluid flow and heat transfer in a lid-driven cavity and analyzed the results for different values of Ri and $Pr = 0.71$. They observed that when $Ri \geq 0$, the stable temperature distribution tends to suppress the vertical fluid motion and as a result much of the fluid motion takes place in the vicinity of the top sliding lid and the bulk of the cavity region is nearly stagnant. Pessa and Piva [14] investigated the influence of Prandtl number and Rayleigh number on average Nusselt number. The study shows that the average Nusselt number increases with the Prandtl number and, in particular, its effect on the Nusselt number is more evident at high Rayleigh numbers. Mohamad and Viskanta [15] they reported on the onset of instability in a shallow lid-driven cavity heated from below. They carried out a linear stability analysis and found that Pr influences the conditions for the initiation of the mixed convection regime. Amiri et al. [16] have analyzed the effects of mixed convection heat transfer in lid-driven cavity with sinusoidal wavy bottom surface. Moallemi and Jang [17] numerically studied mixed convective flow in a bottom heated square driven cavity and investigated the effect of

Prandtl number on the flow and heat transfer process. They found that the effects of buoyancy are more pronounced for higher values of Prandtl number. Mansour and Viskanta [18] studied mixed convective flow in a tall vertical cavity where one of the vertical sidewalls, maintained at a colder temperature than the other, was moving up or downward thus assisting or opposing the buoyancy. They observed that when shear assisted the buoyancy a shear cell developed adjacent to the moving wall while the buoyancy cell filled the rest of the cavity. Oztop and Dagtekin [19] performed numerical analysis of mixed convection in a square cavity with moving and differentially heated sidewalls. Prasad and Koseff [20] performed a series of experiments in a cavity filled with water and measured heat flux at various locations over the hot cavity floor for a range of Re and Gr . However, in the aforementioned works attention has been addressed to the un-tilted geometry, although the inclination effects may be of interest in many science and engineering applications. In fact, as the buoyancy force components change with orientation, transitions between different flow patterns may occur, and the heat transfer rates may change drastically as, e.g., found by Sharif [21] who carried out the analysis of mixed convective flow in a lid-driven inclined shallow rectangular cavity with a top hot lid and cooled from bottom with inclination angle γ in the range between 0° and 30° of aspect ratio 10 with Rayleigh numbers ranging from 10^5 to 10^7 keeping the Reynolds number fixed at 408.21. He found that the local Nusselt number at the heated moving lid starts with a high value and decreases rapidly and monotonically to a small value towards the right side. Chamkha and Al-Naser [22] investigated the double-diffusive convective flow of a binary fluid mixture in inclined square and rectangular cavities. They expanded the range of inclination angle to be from 0° to 90° . Their study was focused on the effect of the buoyancy ratio and the rotation on the evolution of the flow field, temperature and solute field in the cavity. Cianfrini and Corcione [23] expanded the study range of the tilting angle from $0 \leq \gamma \leq 90^\circ$ to $0^\circ \leq \gamma \leq 360^\circ$. It is found for any tilting angle $\gamma < 45^\circ$, the heat transfer rate is the same as that for angle $(90^\circ - \gamma)$. For any tilting angle $\gamma > 225^\circ$, the heat transfer rate is the same as that for angle $(450^\circ - \gamma)$. Benhadji and Vasseur [24] study the Darcy model with the Boussinesq approximations in double diffusive convection in a shallow porous cavity saturated with a non-Newtonian fluid, a power-law model is used to characterize the non-Newtonian fluid behavior. Recently, Teamah et al. [25–29] studied numerically the mixed convection in a rectangular lid-driven cavity under the combined buoyancy effects of thermal and mass diffusion with moving upper surface, both upper and lower surfaces are being insulated and impermeable, constant different temperatures and concentration are imposed along the vertical walls of the enclosure, steady state laminar regime is considered. The transport equations for continuity, momentum, energy and species transfer are solved. The numerical results are reported for the effect of Richardson number, Lewis number, and buoyancy ratio on the iso-contours of stream line, temperature, and concentration. In addition, the predicted results for both local and average Nusselt and Sherwood numbers are presented and discussed for various parametric conditions. This study was done for $0.1 \leq Le \leq 50$ and Prandtl number $Pr = 0.7$. Throughout the study the Grashof number and aspect ratio are kept constant at 10^4 and 2 respectively and $-10 \leq N \leq 10$, while Richardson number has been varied

from 0.01 to 10 to simulate forced convection dominated flow, mixed convection and natural convection dominated flow.

This study is a parametric study and extension of Sharif [21] study. A wide range of buoyancy ratio is studied from $-10 \leq N \leq 10$. In addition, a wide range of Lewis number is studied from $0.1 \leq Le \leq 10$. Moreover, the top lid moves in the upward and downward directions thus the lid-driven shear may be assisting or opposing the buoyancy and the resulting flow. Thermal and mass fields as well as the heat and mass transfer processes will be very different from those of the horizontal configuration case.

2. Mathematical model

The schematic of the systems under consideration is shown in Fig. 1. The cavity sidewalls are adiabatic, the isothermal top and bottom walls are maintained at temperatures T_h and T_c , respectively, with $T_h > T_c$. The aspect ratio of the cavity is defined as $A = L/H$. With this geometry and boundary conditions, the present study reports the computations for cavities at a fixed aspect ratio of 10, and inclination angles ranging from 0° to 30° by tilting the horizontal cavity in counter-clockwise direction. The tilting effect on the heat and species transfer process is analyzed and the results are presented in terms of the streamline, isotherms and isoconcentration plots within the cavity. The variation of the local Nusselt, average Nusselt and Sherwood numbers at the hot surface vs. considered system parameters are presented graphically. The fluid is assumed to be incompressible and Newtonian. The viscous dissipation is neglected. The Boussinesq approximation is given by Eq. (1) with opposite and compositional buoyancy forces are used for the body force terms in the momentum equations:

$$\rho = \rho_\infty [1 - \beta_T(T - T_c) - \beta_s(c - c_l)] \quad (1)$$

The governing equations for the problem under consideration are based on the balance laws of mass, linear momentum, thermal energy and concentration in two dimensions steady state are given as;

$$\frac{\partial u}{\partial x} + \frac{\partial v}{\partial y} = 0 \quad (2)$$

$$u \frac{\partial u}{\partial x} + v \frac{\partial u}{\partial y} = -\frac{1}{\rho} \frac{\partial p}{\partial x} + \nu \left(\frac{\partial^2 u}{\partial x^2} + \frac{\partial^2 u}{\partial y^2} \right) + g \sin \gamma [\beta_T(T - T_c) + \beta_s(c - c_l)] \quad (3)$$

$$u \frac{\partial v}{\partial x} + v \frac{\partial v}{\partial y} = -\frac{1}{\rho} \frac{\partial p}{\partial y} + \nu \left(\frac{\partial^2 v}{\partial x^2} + \frac{\partial^2 v}{\partial y^2} \right) + g \cos \gamma [\beta_T(T - T_c) + \beta_s(c - c_l)] \quad (4)$$

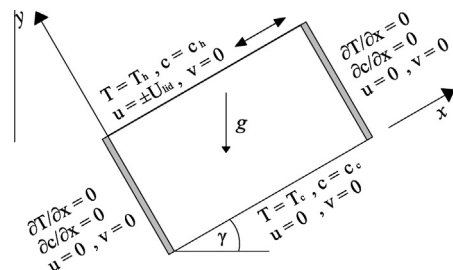


Figure 1 A schematic diagram for the problem.

$$u \frac{\partial T}{\partial x} + v \frac{\partial T}{\partial y} = \alpha \left(\frac{\partial^2 T}{\partial x^2} + \frac{\partial^2 T}{\partial y^2} \right) \quad (5)$$

$$u \frac{\partial c}{\partial x} + v \frac{\partial c}{\partial y} = D \left(\frac{\partial^2 c}{\partial x^2} + \frac{\partial^2 c}{\partial y^2} \right) \quad (6)$$

The boundary conditions are:

- $u = v = 0, \quad T = T_c \quad \text{and} \quad c = c_l, \quad \text{at} \quad y = 0$
 - $u = \pm u_{lid}, \quad v = 0, \quad T = T_h \quad \text{and} \quad c = c_h, \quad \text{at} \quad y = H$
- Positive sign for upward lid moving and negative sign for downward lid moving
- $u = v = \frac{\partial T}{\partial x} = \frac{\partial c}{\partial x} = 0 \quad \text{at} \quad x = 0 \quad \text{and} \quad x = L$

Introducing the following dimensionless groups in the governing equations,

$$\begin{aligned} X &= \frac{x}{H}, \quad Y = \frac{y}{H}, \quad U = \frac{u}{u_{lid}}, \quad V = \frac{v}{u_{lid}}, \\ P &= \frac{p}{\rho_\infty u_{lid}^2}, \quad \theta = \frac{T - T_c}{T_h - T_c}, \quad C = \frac{c - c_l}{c_h - c_l} \end{aligned} \quad (7)$$

The governing equations will be

$$\frac{\partial U}{\partial X} + \frac{\partial V}{\partial Y} = 0 \quad (8)$$

$$\begin{aligned} U \frac{\partial U}{\partial X} + V \frac{\partial U}{\partial Y} = & -\frac{\partial P}{\partial X} + \frac{1}{Re} \left(\frac{\partial^2 U}{\partial X^2} + \frac{\partial^2 U}{\partial Y^2} \right) + \frac{Gr}{Re^2} (\theta \\ & + NC) \sin \gamma \end{aligned} \quad (9)$$

$$\begin{aligned} U \frac{\partial V}{\partial X} + V \frac{\partial V}{\partial Y} = & -\frac{\partial P}{\partial Y} + \frac{1}{Re} \left(\frac{\partial^2 V}{\partial X^2} + \frac{\partial^2 V}{\partial Y^2} \right) + \frac{Gr}{Re^2} (\theta \\ & + NC) \cos \gamma \end{aligned} \quad (10)$$

$$U \frac{\partial \theta}{\partial X} + V \frac{\partial \theta}{\partial Y} = \frac{1}{Re Pr} \left(\frac{\partial^2 \theta}{\partial X^2} + \frac{\partial^2 \theta}{\partial Y^2} \right) \quad (11)$$

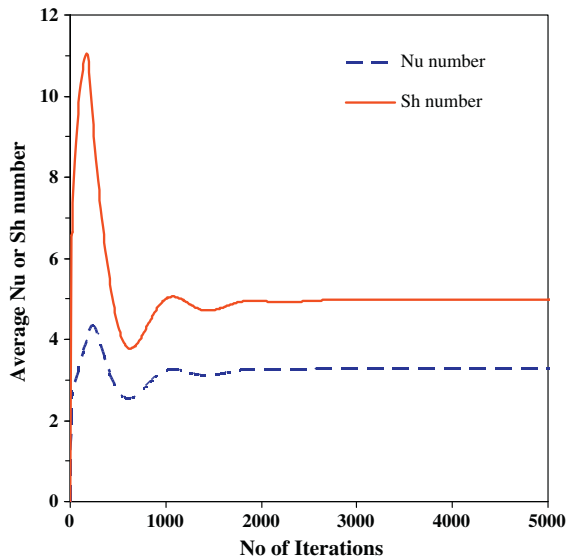


Figure 2 Convergence solution $Ra = 6 \times 10^4, \quad Re = 100, \quad Le = 3, \quad N = 1$ and $\gamma = 10$.

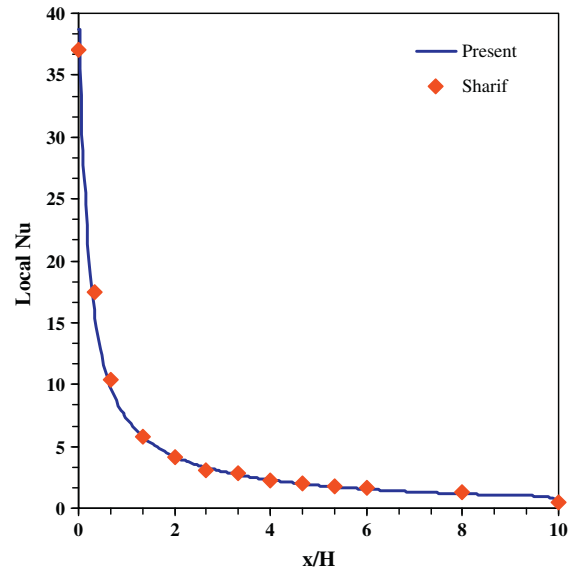


Figure 3 Comparison for local Nusselt number at the hot surface with Sharif [21] results, $Ra = 10^6, \quad Re = 408.21, \quad Pr = 6$ and $\gamma = 0$.

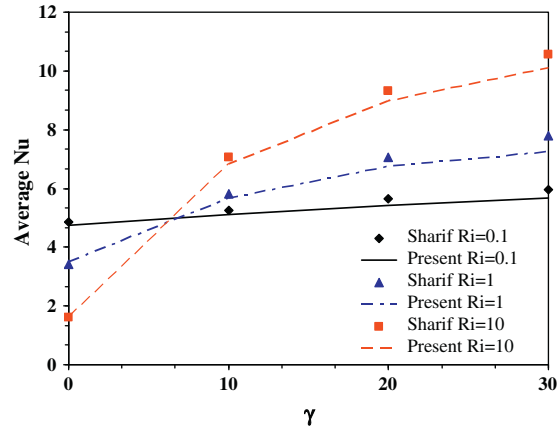


Figure 4 Comparison for average Nusselt number at the hot surface with Sharif [21] results, $Re = 408.21$ and $Pr = 6$.

$$U \frac{\partial C}{\partial X} + V \frac{\partial C}{\partial Y} = \frac{1}{Sc Re} \left(\frac{\partial^2 C}{\partial X^2} + \frac{\partial^2 C}{\partial Y^2} \right) \quad (12)$$

where Re is the Reynolds number, Gr is the Grashof number, N is the buoyancy ratio, Pr is the Prandtl number and Sc is the Schmidt number. The dimensionless boundary conditions are:

- $U = V = \theta = C = 0, \quad \text{at} \quad Y = 0$
- $U = \pm 1, \quad V = 0, \quad \theta = 1 \quad \text{and} \quad C = 1, \quad \text{at} \quad Y = 1$
- $U = V = \frac{\partial \theta}{\partial X} = \frac{\partial C}{\partial X} = 0, \quad \text{at} \quad X = 0 \quad \text{and} \quad X = A = 10$

2.1. Nusselt number calculation

Equating the heat transfer by convection to the heat transfer by conduction at hot wall:

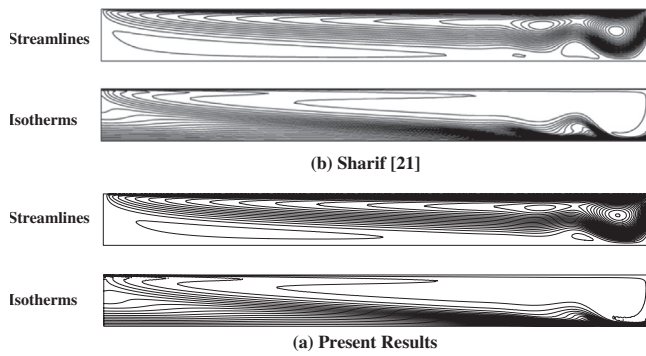


Figure 5 Comparison with Sharif [21], $Ra = 10^6$, $Re = 408.21$, $Pr = 6$ and $\gamma = 0^\circ$.

$$h\Delta T = -k \left(\frac{\partial T}{\partial y} \right)_{y=H} \quad (13)$$

Introducing the dimensionless variables, defined in Eq. (7) into Eq. (13), gives:

$$Nu_x = - \left(\frac{\partial \theta}{\partial Y} \right)_{Y=1} \quad (14)$$

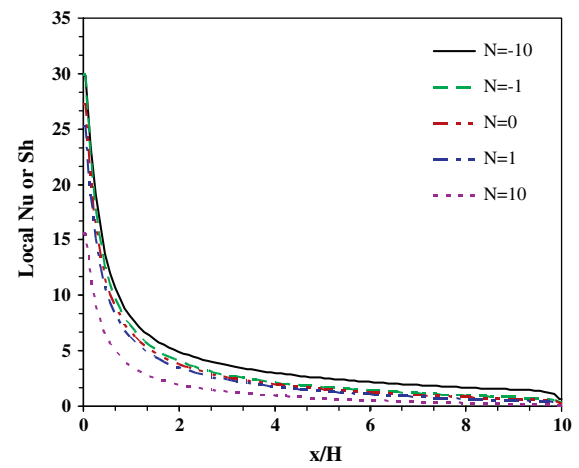


Figure 7 Effect of buoyancy ratio on local Nusselt and Sherwood numbers, $Ra = 6 \times 10^4$, $Re = 100$, $Pr = 6$, $Le = 1$ and $\gamma = 0^\circ$ (upward).

The average Nusselt number is obtained by integrating the above local Nusselt number over the hot wall:

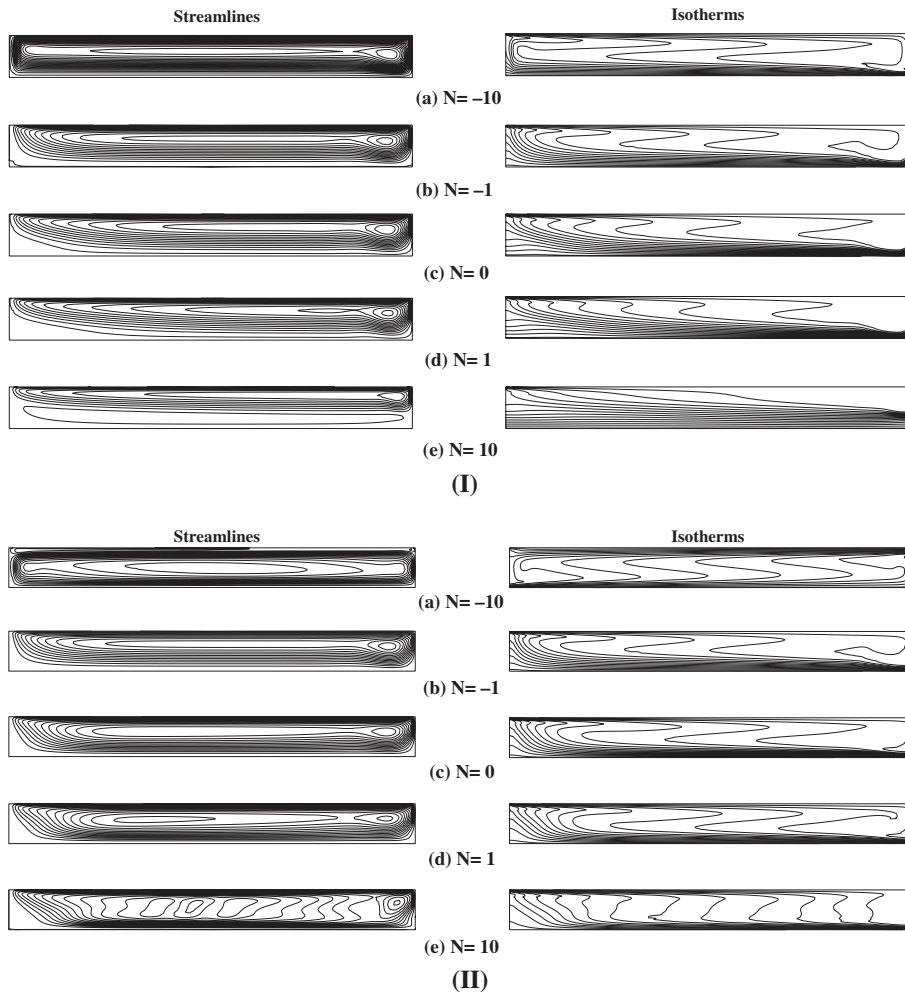


Figure 6 Upward streamlines, isothermal contours for $Ra = 6 \times 10^4$, $Re = 100$, $Pr = 6$, $Le = 1$, (I) $\gamma = 0^\circ$, (II) $\gamma = 30^\circ$.

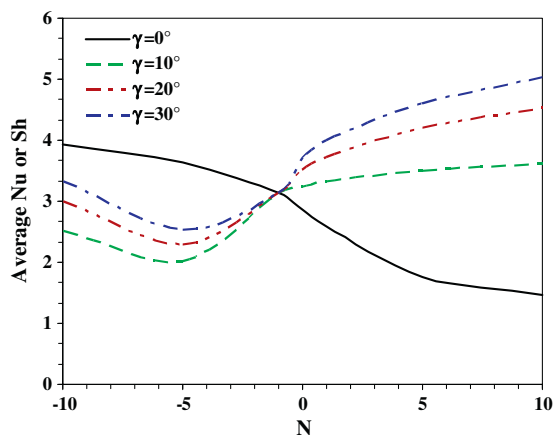


Figure 8 Effect of inclination angle on Average Nusselt and Sherwood Numbers, $Ra = 6 \times 10^4$, $Re = 100$, $Pr = 6$ and $Le = 1$ (upward).

$$Nu = -\frac{1}{A} \int_0^A \left(\frac{\partial \theta}{\partial Y} \right)_{Y=1} dX \quad (15)$$

2.2. Sherwood number calculation

Equating the extracted mass transfer by convection to the added mass transfer to the cavity gives:

$$h_s \Delta c = -D \left(\frac{\partial c}{\partial y} \right)_{y=H} \quad (16)$$

Introducing the dimensionless variables, defined in Eq. (7), into Eq. (16), gives:

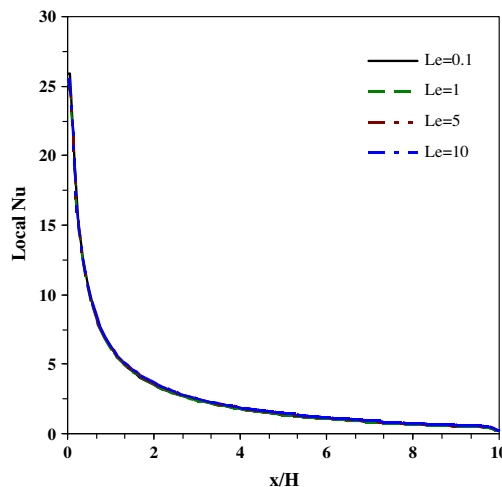


Figure 10 Effect of Lewis number on local Nusselt number, $Ra = 6 \times 10^4$, $Re = 100$, $Pr = 6$, $N = 1$ and $\gamma = 0^\circ$ (upward).

$$Sh_x = -\left(\frac{\partial C}{\partial Y} \right)_{Y=1} \quad (17)$$

The average Sherwood number is obtained by integrating the above local Sherwood number over the hot wall:

$$Sh = -\frac{1}{A} \int_0^A \left(\frac{\partial C}{\partial Y} \right)_{Y=1} dX \quad (18)$$

3. Solution procedure

The governing equations were solved using the finite volume technique developed by Patankar [30]. This technique was based on the discretization of the governing equations using

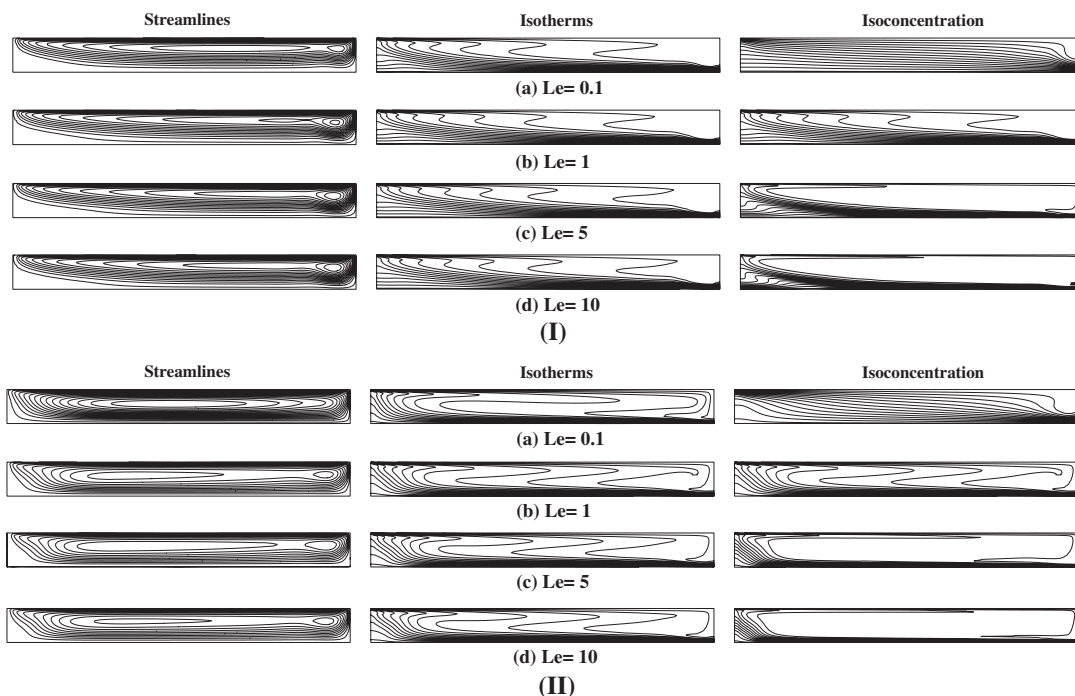


Figure 9 Upward streamlines, isothermal and isoconcentration contours for $Ra = 6 \times 10^4$, $Re = 100$, $Pr = 6$, $N = 1$ (I) $\gamma = 0^\circ$, (II) $\gamma = 30^\circ$.

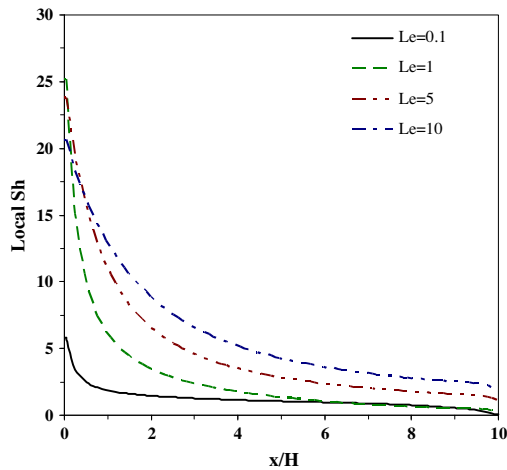


Figure 11 Effect of Lewis number on local Sherwood number, $Ra = 6 \times 10^4$, $Re = 100$, $Pr = 6$, $N = 1$ and $\gamma = 0^\circ$ (upward).

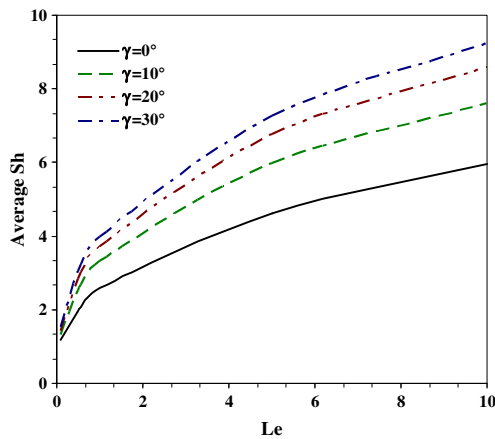


Figure 12 Sherwood number vs. Le for different γ , $Ra = 6 \times 10^4$, $Re = 100$, $Pr = 6$ and $N = 1$ (upward).

the central difference in space using meshing grids (100×40). The discretization equations were solved by the Gauss–Seidel method. The iteration method used in this program is a line-by-line procedure, which is a combination of the direct method and the resulting Tri Diagonal Matrix Algorithm (TDMA). The convergence of the iteration is determined by the change in the average Nusselt and Sherwood numbers as well as other dependent variables through one hundred iterations to be less than 0.001% from its initial value. Fig. 2 shows the convergence and stability of the solution.

4. Program validation and comparison with previous research

In order to check on the accuracy of the numerical technique employed for the solution of the problem considered in the present study, it was validated by performing simulation for mixed convection flow in an inclined cavity with top hot lid moving upward and cold bottom surface is fixed which were reported by Sharif [21]. Fig. 3 plots the predicted values for local Nusselt numbers over the hot surface for the present solution and the results published by Sharif [21]. In the figure, the

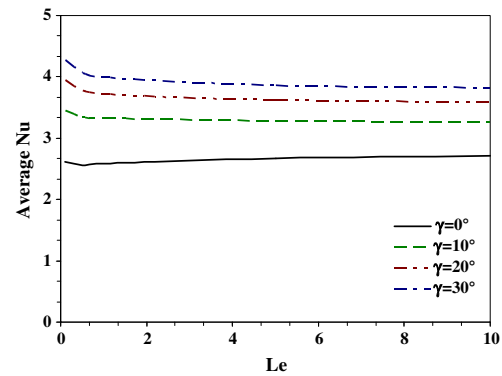


Figure 13 Nusselt number vs. Le for different γ , $Ra = 6 \times 10^4$, $Re = 100$, $Pr = 6$ and $N = 1$ (upward).

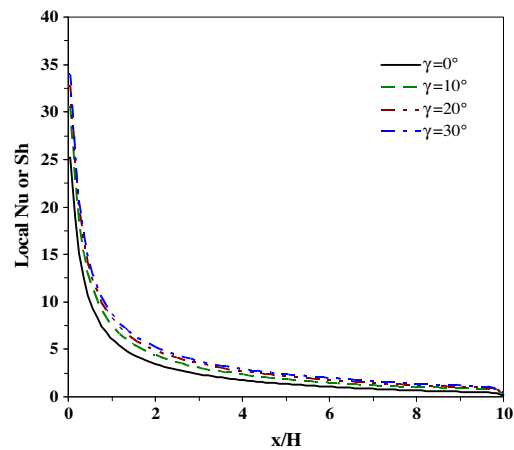


Figure 14 Effect of inclination angle on local Nusselt and Sherwood numbers, $Ra = 6 \times 10^4$, $Re = 100$, $Pr = 6$, $Le = 1$, $N = 1$ (upward).

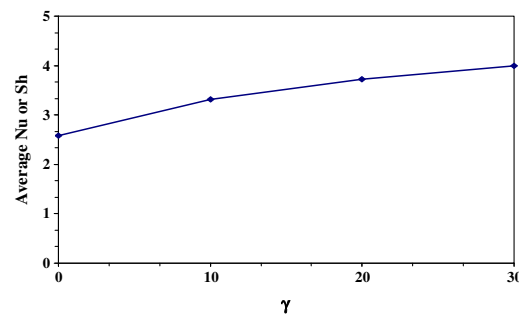


Figure 15 Effect of inclination angle on average Nusselt and Sherwood numbers, $Ra = 6 \times 10^4$, $Re = 100$, $Pr = 6$, $Le = 1$ and $N = 1$ (upward).

inclined angle is equal zero. The following parameters were kept constant $Ra = 10^6$, $Re = 408.21$ and $Pr = 6$. In addition, Fig. 4 plots the values of the average Nusselt number for Rayleigh numbers equal to 10^5 , 10^6 , 10^7 while Reynolds number is kept constant at 408.21 producing corresponding Richardson number of 0.1, 1 and 10. The maximum deviation between the results through this range was within 5%. Some of this

deviation may be from the accuracy in the measuring from the graphs or from the solution techniques. Also, Fig. 5a and b presents comparisons for the streamlines contours of the present work at inclined angle equal zero, $Ra = 10^6$, $Pr = 6$ and $Re = 408.21$ and Sharif [21]. The figure shows good agreement.

5. Results and discussion

In this study, the Rayleigh number is kept constant at $Ra = 6 \times 10^4$, Prandtl number, $Pr = 6$, aspect ratio, $A = 10$ and Reynolds number, $Re = 100$. The numerical results for the streamline, isothermals and isoconcentration contours for various values of Lewis number Le , buoyancy ratio N and inclination angle γ for both hot lid movements will be

presented and discussed. In addition, the results for local, average Nusselt and Sherwood numbers at various conditions will be presented and discussed.

5.1. The hot lid moves upward

5.1.1. Effect of buoyancy ratio

To demonstrate the implications of the negative and positive buoyancy ratio numbers, the isopleths of streamlines and isotherms are plotted in Fig. 6, for different buoyancy ratio. Once more, the Lewis number was set at unity to explore the diffusion characteristics upon varying N thus makes the isoconcentration and isotherms carry out the same contour patterns since they have the same diffusion characteristics at $Le = 1$. A negative value of N indicates that the volumetric expansion

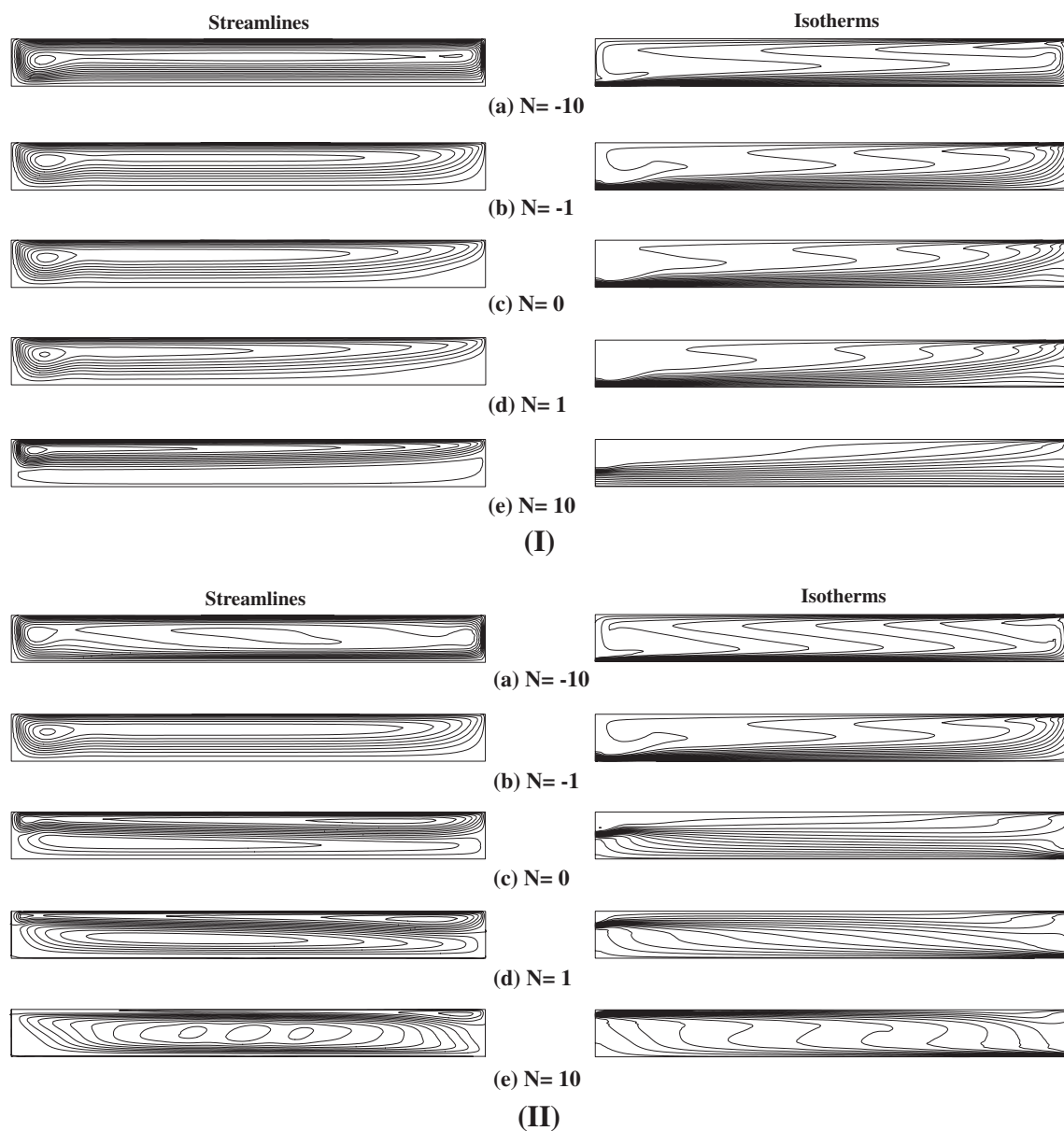


Figure 16 Effect of buoyancy ratio on streamlines and isothermal contours for $Ra = 6 \times 10^4$, $Re = 100$, $Pr = 6$, $Le = 1$, (I) $\gamma = 0^\circ$, (II) $\gamma = 30^\circ$ (downward).

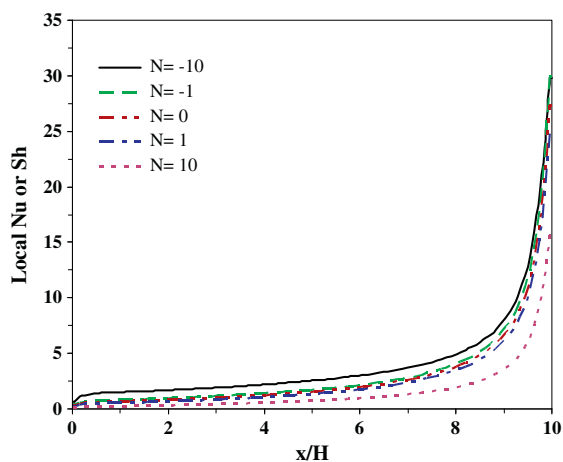


Figure 17 Effect of buoyancy ratio on local Nusselt and Sherwood numbers, $Ra = 6 \times 10^4$, $Re = 100$, $Pr = 6$, $Le = 1$ and $\gamma = 0^\circ$ (downward).

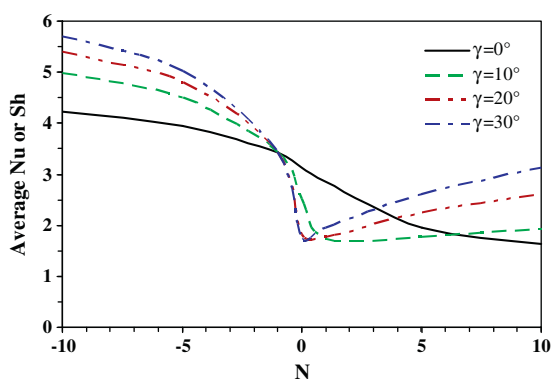


Figure 18 Effect of inclination angle on average Nusselt and Sherwood numbers, $Ra = 6 \times 10^4$, $Re = 100$, $Pr = 6$ and $Le = 1$ (downward).

coefficient with mass fraction (β_s) holds a negative value for the prescribed temperature range. At $N = -10$ (dominant mass transfer regime), the flow field is characterized by a primary clockwise circulating bubble near the right-hand wall where the shear driven flow by the lid is impacted on the side-wall and is forced to move downward. In all cases a thin hydrodynamic and thermal boundary layer is observed at the heated top moving lid. The isotherms show that the fluid is vertically stratified in the stagnant zone and conduction is the principal mode of heat transfer in that zone. Further increase of N , the primary bubble moves upward and the flow is almost stagnant in the left lower corner introducing a counter clockwise vortex increase till $N = 10$. Also by increasing the buoyancy ratio, the isotherms depreciate at the top that makes the region of conduction increases and decreasing the pure natural convection in the right top corner. The cavity inclination has significant impact on the thermal and hydrodynamic flow fields. The lower reverse vortex intensity increases and main bubble was divided into two small vortices in the top corners. It is noticed that, when N equal -1 the reverse flow diminished the primary bubble regain its intensity. Further increase in N , a

second vortex built up in the center of cavity and its intensity increased until it is broken up at $N = 10$ when γ equals 30° . While the isotherms clarify two stratified layers of conduction at the top and bottom surfaces of the cavity, as N increases, the top layers go down to form a thin thermal boundary layer at bottom with its intensity decreases as γ increases.

The variation of the local Nusselt and Sherwood numbers along the hot moving lid are plotted in Fig. 7. In general, the Nusselt and Sherwood numbers at the hot lid start with high values at the left end and they decrease monotonically to small values towards the right end. It is found when the buoyancy ratio number increases both the local Nusselt and Sherwood numbers decrease. The effect of buoyancy ratio number on the average values of Nusselt and Sherwood numbers is illustrated in Fig. 8. As is shown both of the average numbers decrease as N increases till $N = -5$, after that they increase to reach their highest values at $N = 10$ except for $\gamma = 0^\circ$ they decrease continuously.

5.1.2. Effect of Lewis number

The dependence of heat and species transport on the Lewis number is displayed in Fig. 9. The Lewis number provides a measure of thermal diffusivity of a fluid to its mass diffusivity. Thus, a large value of Lewis number reflects a relatively low mass diffusivity value. The Lewis number in the ongoing investigation was varied in the range from 0.1 to 10. In addition, the system parameters Ra , Re and N were taken fixed at 6×10^4 , 100 and 1, respectively. At $Le = 0.1$, the mass diffusion rate appears to be stratified in the vertical direction except at the top right corner due to the circulation of flow caused by the moving lid. The isoconcentration and isotherms carry out the same contour patterns since they have the same diffusion characteristics at $Le = 1$. ‘Concentration’ plumes are observed to emerge below the hot lid, in addition, thinner solutal boundary layers are observed to cluster under the hot lid and above the cold surface, which indicate a substantial increase in the mass transfer rate. This observation is further manifested as Le value was elevated to 10 (dominant mass transfer regime). In other words, the basic mass flow patterns show depreciation in its intensity with the increase in Le value. Furthermore, the results also point out that the effect of Le on the isotherms seems to be insignificant for $Le \geq 1$ as displayed in Fig. 10. For $Le < 1$, however, the thermal plumes tend to ease a bit with the increase in Le value. The variation of the local Nusselt and Sherwood numbers along the hot moving lid is plotted in Figs. 10 and 11. In general, the local Nusselt number has no improvement as Lewis number increases while the local Sherwood number increases when Lewis number increases. The influence of Lewis number on the average value of Sherwood number is presented in Fig. 12. The increase in the prediction of Sherwood number is divided as Le is increased (dominant mass transfer regime) or the tilting angle increase as well. On the contrary, in Fig. 13 the Nusselt number predictions show a slight dip and then assume an asymptotic value with the increase in Le . Unlike the mass transfer enhancement, the transport of energy is not improved with the increase in Le value. Again, the predictions of the Nusselt and Sherwood numbers are coincided at $Le = 1$ giving the similarity in their diffusion characteristics. The local and overall values of Nusselt and Sherwood numbers at the hot surface, which are a measure of the local and overall heat and mass transfer rate, are plotted in Figs. 14 and 15 as a function of the cavity inclination, the

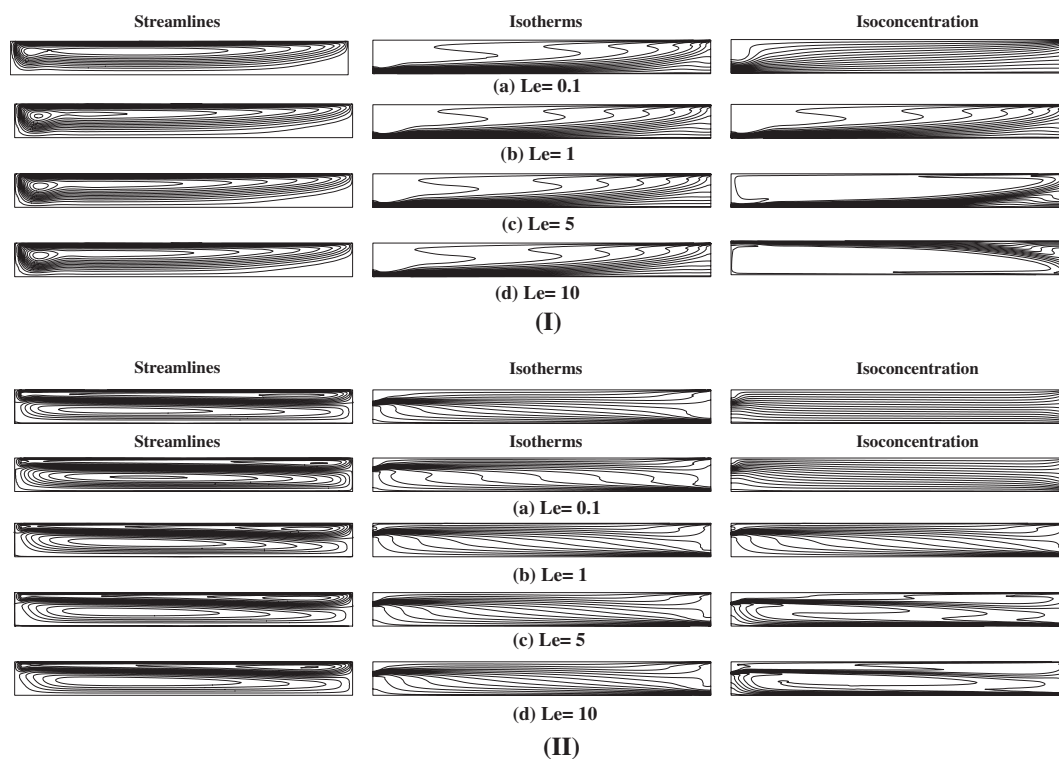


Figure 19 Effect of Lewis number on streamlines, isothermal and isoconcentration contours for $Ra = 6 \times 10^4$, $Re = 100$, $Pr = 6$, $N = 1$, (I) $\gamma = 0^\circ$, (II) $\gamma = 30^\circ$ (downward).

average values increase mildly with the cavity inclination. In addition, at any location both the local Nusselt and Sherwood numbers increase with the cavity inclination.

5.2. The hot lid moves downward

The effect of the lid reverse direction and its influence on the isopleths, heat and mass transfer is explored next. The effect of buoyancy ratio number on flow field and isotherms is shown in Fig. 16. In which the flow field is characterized by a primary counter clockwise circulating bubble near the left hand wall and is forced downward due to the lid movement. By increasing N a stagnant flow is built up in the right lower corner, this flow extends to cover the bottom surface and lift the main circulating flow. The inclination angle increment plays a very important role in increasing the intensity of stagnant flow and due to the main recirculation, the quiescent flow change to a vortex begins to rotate in the clockwise direction. This vortex has the highest intensity at angle 30° and $N = 10$. Meanwhile, the isotherms show that when $N = -10$ (dominant mass transfer regime), the thermal plumes represent a high value of heat transfer by convection which is decreased as N increases. At $N = 10$ the fluid is vertically stratified in the stagnant zone and conduction is the principal mode of heat transfer in that zone. Also in the isotherms, the angle increment demonstrate a dominant convection effect at $N = -10$ which overrules the cavity space, except two thermal boundary layers of conduction beside the top and bottom surfaces and these layers are increased as N increases.

The variation of the local Nusselt and Sherwood numbers along the hot moving lid is plotted in Fig. 17. In general, the

Nusselt and Sherwood numbers at the hot lid start with a small value at the left end and increase monotonically to a high value towards the right end which is opposite to what exists in the first case and by increasing N both local values decrease. The effect of buoyancy ratio number on the average values of Nusselt and Sherwood numbers is illustrated in Fig. 18. Both of average numbers decrease as N increases till $N = 0$ after that they increase to reach their highest values at $N = 10$ except for $\gamma = 0^\circ$ they decrease continuously.

5.2.1. Effect of Lewis number

Next, the influence of Lewis number on heat and species transfer is presented in Fig. 19. Similar to the first case, the mass diffusion rate appears to be stratified in the vertical direction except the top left corner at lower Lewis number values as the inclined angle increase the stratums filled whole cavity. The increment in Lewis number leads to develop concentration plumes increases substantially as Lewis value was elevated to 10 (dominant mass transfer regime). Furthermore, the results point out that the effect of Le on the isotherms seems to be insignificant for $Le \geq 1$ as displayed in Fig. 19. For $Le < 1$, however, the thermal plumes tend to ease a bit with the increase in Le value. Also the cavity inclination has significant impact on the thermal and hydrodynamic flow fields. By increasing the tilting angle to the main circulating bubble approach the top lid and a lower reverse vortex flow which intensity increases with the angle increases. Meanwhile the isotherms show that as γ increases the thickness of stratified layer of conduction which emerge the bottom surface increases to fill the lower half of the cavity. When angle value was elevated to 30° , the conduction layer divides into a thick layer

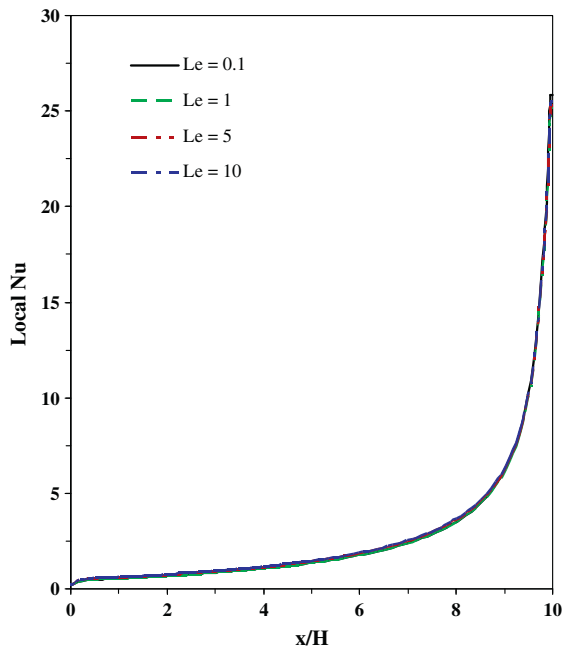


Figure 20 Effect of Lewis number on local Nusselt number, $Ra = 6 \times 10^4$, $Re = 100$, $Pr = 6$, $N = 1$ and $\gamma = 0^\circ$ (downward).

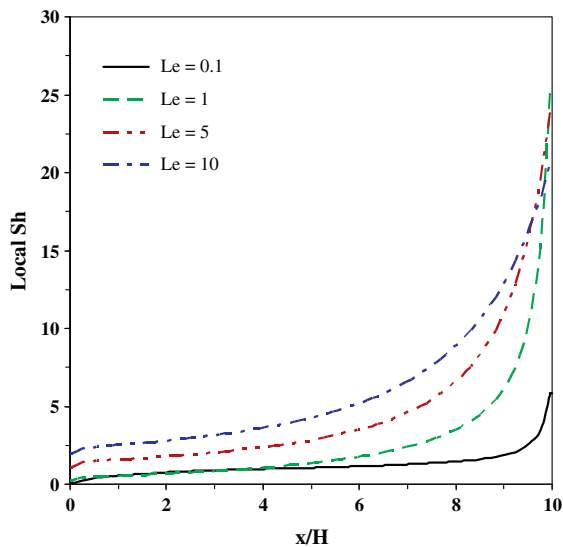


Figure 21 Effect of Lewis number on local Sherwood number, $Ra = 6 \times 10^4$, $Re = 100$, $Pr = 6$, $N = 1$ and $\gamma = 0^\circ$ (downward).

cover the top lid and a thin layer cover the bottom surface which signal to an increment in the convection heat transfer.

The effect of Lewis number on both local Nusselt and Sherwood numbers is illustrated in Figs. 20 and 21. In general, the local Nusselt number has no improvement as Lewis number increases while the local Sherwood number increases when Lewis number increases just like the case of the upward lid motion. The influence of Lewis number on the average values of Nusselt and Sherwood numbers appears in Figs. 22 and 23 the Nusselt number is independent on Lewis number unlike

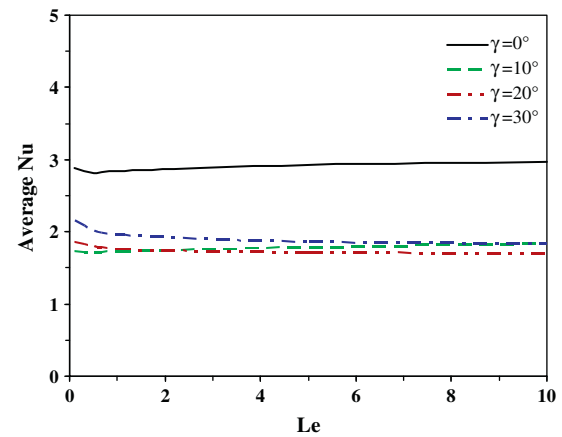


Figure 22 Nusselt number vs. Le for different γ , $Ra = 6 \times 10^4$, $Re = 100$, $Pr = 6$ and $N = 1$ (downward).

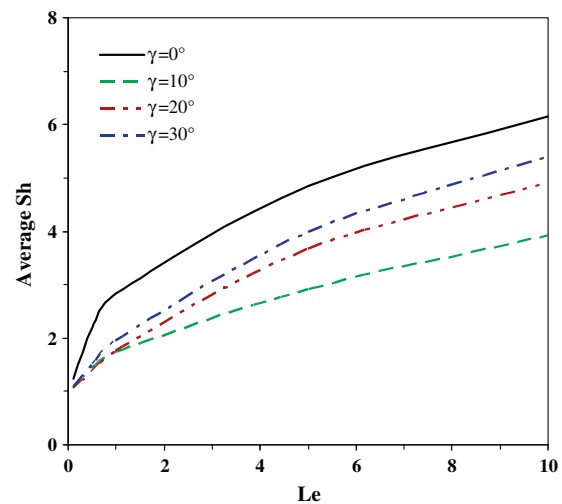


Figure 23 Sherwood number vs. Le for different γ , $Ra = 6 \times 10^4$, $Re = 100$, $Pr = 6$ and $N = 1$ (downward).

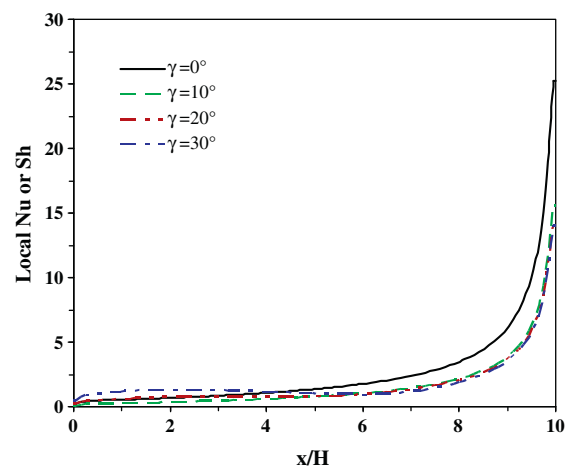


Figure 24 Effect of inclination angle on local Nusselt and Sherwood numbers, $Ra = 6 \times 10^4$, $Re = 100$, $Pr = 6$, $Le = 1$, $N = 1$ (downward).

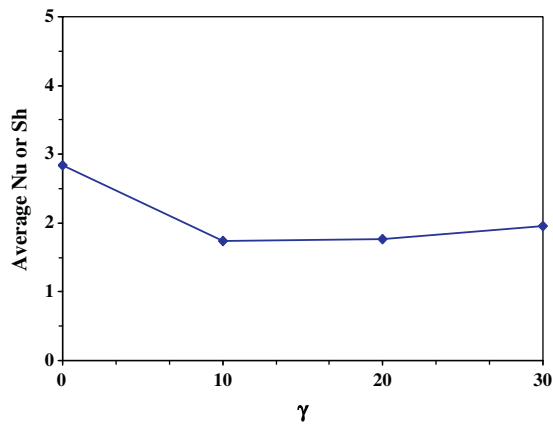


Figure 25 Effect of inclination angle on average Nusselt and Sherwood numbers, $Ra = 6 \times 10^4$, $Re = 100$, $Pr = 6$, $Le = 1$ and $N = 1$ (downward).

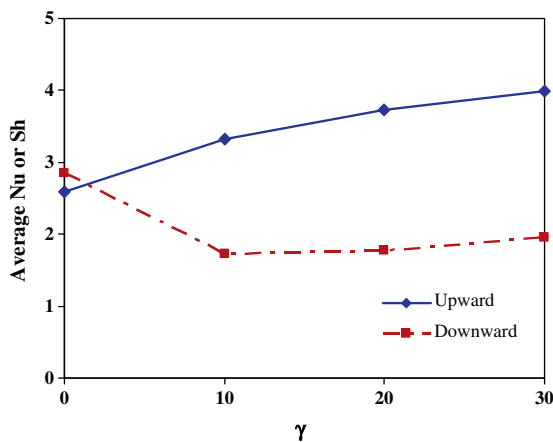


Figure 26 Comparison between upward and downward movements for average Nusselt and Sherwood numbers, $Ra = 6 \times 10^4$, $Re = 100$, $Pr = 6$, $Le = 1$ and $N = 1$.

Sherwood number which is vivid as Lewis number increases. Furthermore, the increments of inclination angle causes decrease in both local and average values of Nusselt and Sherwood numbers as illustrated in Figs. 24 and 25. They have the highest values at $\gamma = 0^\circ$ and by increasing γ the values drop till $\gamma = 10^\circ$ then their values increase mildly. Fig. 26 shows a comparison between the upward and downward top lid movements and the effect of the inclination on both the average Nusselt and Sherwood numbers. It is noticed that the values of average Nusselt or Sherwood numbers for the upward movement case are higher than of those for the downward movement case at all considered inclination angles except the horizontal case the reverse is found.

6. Conclusions

The current investigation is concerned with the numerical simulation of double diffusive flow in a two dimensional shallow inclined driven cavity with the top lid moves in both upward and downward directions. The Patankar–Spalding technique was used to solve the set of the governing equations. The

investigation was carried out for a broad spectrum of relevant dimensionless groups to explore their effects on the overall flow patterns and transport rates. The employed domains of these dimensionless groups were as follows: $0.1 \leq Le \leq 10$ and $-10 \leq N \leq 10$. The results show that the flow field is characterized by a primary circulating bubble with its place depends on the direction of the moving lid. Furthermore, high Le values significantly improve the mass transfer rate, whereas Le is found to have insignificant impact on the heat transfer rate. Also, the increase in the absolute value of the buoyancy ratio number N was found to enhance the estimated Nusselt number and the Sherwood number for both cases of lid movements. Next, the tilting effect on heat and species transfer is studied, the increment in the inclination angle leads to increase both values of the Nusselt and Sherwood numbers mildly for the upward movement case. On the contrary, in the downward movement case they decrease at first till $\gamma = 10^\circ$ afterwards they start to increase as the angle increases. It is noticed that the values of the average Nusselt or Sherwood numbers in the first case are higher than of those of the second case. The results of the present work may play an important role on enhancing the performance of many engineering applications such as crystal growth which is important in fabrication of infrared detectors, memory devices, and integrated circuits.

References

- [1] Y. Masuda, A. Suzuki, Y. Mikawa, C. Yokoyama, T. Tsukada, Numerical simulation of natural convection heat transfer in a ZnO single-crystal growth hydrothermal autoclave – effects of fluid properties, *J. Crystal Growth* 311 (2009) 675–679.
- [2] L.B. Wang, N.I. Wakayama, W.Q. Tao, The role of solutal convection in protein crystal growth – a new dimensionless number to evaluate the effects of convection on protein crystal growth, *J. Crystal Growth* 310 (2008) 5370–5374.
- [3] M. Yang, N. Ma, A computational study of natural convection in a liquid-encapsulated molten semiconductor with a horizontal magnetic field, *Int. J. Heat Fluid Flow* 26 (2005) 810–816.
- [4] N. Ma, J.S. Walker, A parametric study of segregation effects during vertical Bridgman crystal growth with an axial magnetic field, *J. Crystal Growth* 208 (2000) 757–771.
- [5] S. Chakraborty, P. Dutta, Three-dimensional double-diffusive convection and macrosegregation during non-equilibrium solidification of binary mixtures, *Int. J. Heat Mass Transfer* 46 (2003) 2115–2134.
- [6] B. Rudels, G. Björk, R.D. Muench, U. Schauer, Double-diffusive layering in the Eurasian basin of the Arctic ocean, *J. Mar. Syst.* 21 (1999) 3–27.
- [7] J.M. Hyun, J.W. Lee, Double-diffusive convection in a rectangle with cooperating horizontal gradients of temperature and concentration, *Int. J. Heat Mass Transfer* 33 (1990) 1605–1617.
- [8] M.M. Ganzarolli, L.F. Milanez, Natural convection in rectangular enclosures heated from below and symmetrically cooled from the sides, *Int. J. Heat Mass Transfer* 38 (1995) 1063–1073.
- [9] T. Basak, S. Roy, A.R. Balakrishnan, Effects of thermal boundary conditions on natural convection flows within a square cavity, *Int. J. Heat Mass Transfer* 49 (2006) 4525–4535.
- [10] D.C. Loa, D.L. Young, C.C. Tsai, High resolution of 2D natural convection in a cavity by the DQ method, *J. Comput. Appl. Math.* 203 (2007) 219–236.
- [11] V.A.F. Costa, Double diffusive natural convection in a square enclosure with heat and mass diffusive walls, *Int. J. Heat Mass Transfer* 40 (1997) 4061–4071.

- [12] O. Aydın, A. Unal, T. Ayhan, Natural convection in rectangular enclosures heated from one side and cooled from the ceiling, *Int. J. Heat Mass Transfer* 42 (1999) 2345–2355.
- [13] R. Iwatsu, J.M. Hyun, Three dimensional driven cavity flows with a vertical temperature gradient, *Int. J. Heat Mass Transfer* 38 (1995) 3319–3328.
- [14] T. Pessa, S. Piva, Laminar natural convection in a square cavity: low Prandtl numbers and large density differences, *Int. J. Heat Mass Transfer* 52 (2009) 1036–1043.
- [15] A.A. Mohamad, R. Viskanta, Stability of lid-driven shallow cavity heated from below, *Int. J. Heat Mass Transfer* 32 (1989) 2155–2166.
- [16] A.M. Al-Amiri, K.M. Khanafer, I. Pop, Effect of sinusoidal wavy bottom surface on mixed convection heat transfer in a lid driven cavity, *Int. J. Heat Mass Transfer* 50 (2007) 1771–1780.
- [17] M.K. Moallemi, K.S. Jang, Prandtl number effects on laminar mixed convection heat transfer in a lid-driven cavity, *Int. J. Heat Mass Transfer* 35 (1992) 1881–1892.
- [18] R.B. Mansour, R. Viskanta, Shear-opposed mixed-convection flow and heat transfer in a narrow, vertical cavity, *Int. J. Heat Fluid Flow* 15 (1994) 462–469.
- [19] H.F. Oztop, I. Dagtekin, Mixed convection in two-sided lid-driven differentially heated square cavity, *Int. J. Heat Mass Transfer* 47 (2004) 1761–1769.
- [20] A.K. Prasad, J.R. Koseff, Combined forced and natural convection heat transfer in a deep lid-driven cavity flow, *Int. J. Heat Fluid Flow* 17 (1996) 460–467.
- [21] M.A.R. Sharif, Laminar mixed convection in shallow inclined driven cavities with hot moving lid on top and cooled from bottom, *Appl. Therm. Eng.* 27 (2007) 1036–1042.
- [22] A.J. Chamkha, H. Al-Naser, Double-diffusive convection in an inclined porous enclosure with opposing temperature and concentration gradients, *Int. J. Therm. Sci.* 40 (2001) 227–244.
- [23] C. Cianfrini, M. Corcione, Natural convection in tilted square cavities with differentially heated opposite walls, *Int. J. Heat Mass Transfer* 44 (2005) 441–451.
- [24] K. Benhadji, P. Vasseur, Double diffusive convection in a shallow porous cavity filled with a non-Newtonian fluid, *Int. Commun. Heat Mass Transfer* 28 (2001) 763–772.
- [25] M.A. Teamah, W.M. El-Maghlany, Numerical simulation of double-diffusive convective flow in differentially heated rectangular enclosure with insulated moving lid on top, *Int. J. Therm. Sci.* 49 (9) (2010) 1625–1638.
- [26] Mohamed A. Teamah, Ahmad F. Elsafty, Enass Z. Massou, Numerical simulation of double-diffusive natural convective flow in an inclined rectangular enclosure in the presence of magnetic field and heat source, *Int. J. Therm. Sci.* 52 (2012) 161–175.
- [27] M.A. Teamah, M.M. Abo Elazm, A. Zaki, Numerical study of mixed convection heat transfer and fluid flow in cubical lid-driven cavity, *Eur. J. Sci. Res.* 72 (3) (2012) 460–473.
- [28] Mohamed M. Khairat Dawood, Mohamed A. Teamah, Hydro-magnetic mixed convection double diffusive in a lid driven square cavity, *Eur. J. Sci. Res.* 85 (3) (2012) 336–355.
- [29] M.A. Teamah, W.M. El-Maghlany, Augmentation of natural convective heat transfer in square cavity by utilizing nanofluids in the presence of magnetic field and uniform heat generation/absorption, *Int. J. Therm.* 58 (2012) 130–142.
- [30] S.V. Patankar, *Numerical Heat Transfer and Fluid Flow*, McGraw-Hill, New York, 1980.